Title
Reliability and validity of a MR-based volumetric analysis of the intrinsic foot muscles

Journal
Journal of Magnetic Resonance Imaging, 38(5)

ISSN
1053-1807

Authors
Cheuy, Victor A
Commean, Paul K
Hastings, Mary K
et al.

Publication Date
2013-11-01

DOI
10.1002/jmri.24069

Peer reviewed

HHS Public Access

Author manuscript

J Magn Reson Imaging. Author manuscript; available in PMC 2015 April 17.

Published in final edited form as:

J Magn Reson Imaging. 2013 November ; 38(5): 1083–1093. doi:10.1002/jmri.24069.

Reliability and Validity of a Magnetic Resonance-Based Volumetric Analysis of the Intrinsic Foot Muscles

Victor A. Cheuy, MS[1] **[PhD Student]**, **Paul K. Commean, BEE**[2] **[Research Instructor]**, **Mary K. Hastings, PT, DPT**[3] **[Assistant Professor]**, and **Michael J. Mueller, PT, PhD**[4] **[Professor]**

[1]Applied Biomechanics Laboratory, Movement Science Program, and Program in Physical Therapy, Washington University School of Medicine, St. Louis, Missouri, USA

[2]Electronic Radiology Laboratory, Mallinckrodt Institute of Radiology, Washington University School of Medicine, St. Louis, Missouri, USA

[3]Program in Physical Therapy, Washington University School of Medicine, St. Louis, Missouri, USA

[4]Applied Biomechanics Laboratory, Movement Science Program, Program in Physical Therapy, and Department of Radiology, Washington University School of Medicine, St. Louis, Missouri, USA

Abstract

Purpose—To describe a semi-automated program that will segment subcutaneous fat, muscle, and adipose tissue in the foot using magnetic resonance (MR) imaging, determine the reliability of the program between and within raters, and determine the validity of the program using MR phantoms.

Materials and Methods—MR images were acquired from 19 subjects with and without diabetes and peripheral neuropathy. Two raters segmented and measured volumes from single MR slices at the forefoot, midfoot, and hindfoot at two different times. Intra and inter-rater correlation coefficients were determined. Muscle and fat MR phantoms of known volumes were measured by the program.

Results—Most ICC reliability values were over 0.950. Validity estimates comparing MR estimates and known volumes resulted in r^2 values above 0.970 for all phantoms. The root mean square error was less than 5% for all phantoms.

Conclusion—Subcutaneous fat, lean muscle, and adipose tissue volumes in the foot can be quantified in a reliable and valid way. This program can be applied in future studies investigating the relationship of these foot structures to functions in important pathologies including the neuropathic foot or other musculoskeletal problems.

Keywords

Diabetes mellitus; peripheral neuropathy; intermuscular adipose tissue; muscle

Corresponding Author: V.A.C., Movement Science Program, and Program in Physical Therapy, Washington University School of Medicine, Campus Box 8502, 4444 Forest Park Ave., St. Louis, MO 63108. Phone: 314-286-1441. cheuyv@wusm.wustl.edu.

Introduction

There are over 25 million people with diabetes mellitus (DM) in the United States, and 60-70% of them have some level of neuropathy (1). Motor neuropathy results in substantial lower extremity muscle weakness that is worse distally in the foot than proximally in the calf (2, 3). The loss of muscle function in the intrinsic foot muscles is thought to contribute to foot deformity, which has been associated with forefoot skin breakdown and amputation (3-6). Primary functions of the intrinsic foot muscles are to provide dynamic stability to support the longitudinal arches and the metatarsophalangeal joint (MPJ) (3, 4, 6). Neuropathy and the associated infiltration of intermuscular adipose tissue (IMAT) in these muscles lead to their weakness. IMAT is defined as the adipose tissue beneath the muscle fascia, between muscles, or within muscles, and it is associated with insulin resistance and an increased risk of metabolic impairments (7-10). Intrinsic foot muscle weakness can lead to a muscular imbalance between the denervated intrinsic foot muscles that flex the MPJ and the innervated extrinsic toe extensor muscles contributing to MPJ hyperextension and interphalangeal flexion, commonly called hammer or claw toe (3, 11). Intrinsic foot muscle weakness may also contribute to foot alignment changes, such as the collapse of the arch in medial column deformity (3, 12, 13). However, these relationships are complex and not fully understood (4, 6).

The ability to measure the ratio of IMAT to lean muscle volume in the intrinsic foot muscles would help to predict muscle function (14, 15). Sensory nervous system deficits from DM and peripheral neuropathy (PN) have been well documented, and previous studies have shown its direct correlation with motor deficits and muscle weakness in the distal extremities (2, 3). Therefore, the weakened, neuropathic intrinsic foot muscles would be expected to experience the most severe muscle mass loss and IMAT gain. Magnetic resonance imaging (MRI) is a non-invasive approach to quantitatively measure these foot structures because it can provide high-contrast-resolution imaging of soft tissues in multiple planes (16). Volume estimation of IMAT using MRI has been investigated in the upper extremities, abdomen, liver, and calf, but not in the foot (2, 7, 8, 17-24). A highly reliable, validated method that enables semi-automated, quantitative analyses of lean muscle and IMAT volumes in the intrinsic foot muscles has not been established, and would allow researchers to measure differences between or within groups of subjects over time to identify how intrinsic foot muscles contribute to muscle weakness and joint deformity.

The purposes of this study are to 1) describe a semi-automated program that will segment subcutaneous fat and intrinsic foot muscles based on signal intensities of a MR image, 2) determine the reliability of the program to quantify lean muscle and IMAT volumes at the forefoot, midfoot, and hindfoot, and 3) determine the validity of the program using MR phantoms composed of known proportions of lean meat and fat. It was hypothesized that the intraclass correlation coefficients (ICC) indicating intra- and interrater reliability for the measures would be greater than 0.950, that there would be a strong, linear relationship ($r^2 > 0.950$) between the MR phantoms' volumes measured by the program and by water displacement, and the root mean square error (RMSE) between measures would be less than 5%.

Materials and Methods

Subjects

MR images from 19 adult subjects were used in this study (9 men, 10 women; age 56 ± 12 years). 12 of the subjects had DM and PN (age 57 ± 12 years), 6 of whom also had medial column deformity (i.e. met 2 of the following criteria: calcaneal eversion ≥ 5°, arch angle < 130°, navicular height ≤ 24 mm, and medial column peak plantar pressure > 29 N/cm^2). The remaining 7 subjects were control subjects without DMPN or deformity (age 53 ± 12 years). The complete demographic summary is shown in Table 1. The subjects were recruited from two ongoing studies and informed consent was obtained from each subject. Inclusion criteria for the DMPN group were type 1 or 2 DM and the inability to sense a 5.07 Semmes-Weinstein monofilament on at least one spot on the plantar foot (25). Inclusion criteria for the control group were no history of DM or PN, no presence of foot deformity, and the ability to sense the 5.07 monofilament everywhere on the plantar foot. Exclusion criteria for all subjects included the presence of metal implants, lower extremity amputations greater than digits only, and a weight of 400 lbs or more. Subjects with and without diabetes, and with and without foot deformity were selected to provide a wide range of IMAT and lean muscle volumes, and varying difficulties of anatomical landmark identification.

Image Acquisition

The coronal plane MR images of the subjects were collected using established methods on a Siemens Magnetom Trio 3T scanner (Siemens Medical Systems, Malvern, PA) (8). The subjects were placed in a supine position with the target foot perpendicular to the table. A Siemens head coil was placed over the target foot to obtain the highest resolution without sacrificing the signal strength / noise ratio. The target foot for the DMPN+deformity subjects was the foot with deformity, and was the right foot for all other subjects. Image acquisition for the MR phantoms used the same coil with slices taken perpendicular to the patient table. Subjects' data were obtained from two different studies using two different sets of MR parameters. The following MR parameters were used for 8 of the subjects and the MR phantoms: spin echo pulse sequence, TR/TE = 700/11 msec, field of view = 120 mm, bandwidth = 244 Hz/pixel, 65 slices, thickness = 3.5 mm, transverse orientation, signal averages = 1, flip angle = 128°, matrix = 320 × 320, echo train length = 4, acquisition time ≈ 9 minutes, and pixel size 0.375 × 0.375 mm. The following MR parameters were used for the remaining 11 subjects: spin echo pulse sequence, TR/TE = 5360/38 msec, field of view = 140 mm, bandwidth = 181 Hz/pixel, 35 slices, thickness = 3.5 mm, transverse orientation, signal averages = 1, flip angle = 141°, matrix = 384 × 384, echo train length = 9, acquisition time ≈ 12 minutes, and pixel size 0.365 × 0.365 mm. Both sequences were optimized to image fat, but the latter was also optimized to image tendon. Expert radiologist opinion did not expect, nor did visual examination reveal, noticeable differences in fat and muscle signal intensities in images using the two different MR sequences.

Segmentation Methods

Methods to segment specific muscle and fat volumes have been previously reported for the calf (8). These methods were developed and automated further into a new program and applied to structures in the foot for use as a research tool. The MatLab (Mathworks, Natick,

MA) program requires MR images in the AnalyzeImage 7.5 format. A histogram of all voxel intensities is produced from the inputted slice. A new feature of this program is that multiple Gaussian functions are fit to the histogram to determine the threshold between muscle and fat corresponding to the minimum between the peaks of the two tissue types or their intersection point of overlap, as determined by conditions programmed into the function (Fig. 1). The threshold is calculated on an individual subject basis, unique to each MR image. Given the dramatic infiltration of adipose tissue into the intrinsic foot muscles of the neuropathic foot and the occasional visual blurring of muscle and adipose tissues, automatic threshold detection is critical to allow objective separation between the lean and fat tissues (Fig. 2). The volume measurements were calculated utilizing the threshold automatically identified from the intensities in the MR image (Fig. 1a,b). A low intensity threshold of 51 was determined from the validity testing, and set to eliminate any partial volume effects due to air occurring over the thickness of the slice due to image resolution (Fig. 1c,d). An edge detection algorithm based on the derivative of intensities was used to determine the borders between subcutaneous fat, and the intrinsic muscles (Fig. 3d-i). Manual editing of these borders, optional in the forefoot slices and necessary in the midfoot and hindfoot slices, was performed using Microsoft Paint (Redmond, WA). The remaining volume corresponding to the intrinsic foot muscles was selected by the user (Fig. 3j-l), and separated into muscle and pure fat volumes as determined by the automated threshold (Fig. 4). If the muscle and pure fat volume images were determined to be inaccurate based on visual comparisons to the original MR image, the user adjusted the threshold, and the muscle and IMAT volumes were recalculated and updated accordingly.

Reliability Methods

A biomedical engineer trained in anatomy (rater 1) and an electrical engineer in radiology (rater 2) served as raters. Engineers served as raters for this research tool because they were responsible for developing and using the program. Their lack of clinical training highlights the ability of the program to be used by those who are not radiologists or clinicians. The raters met with radiologists on 3 occasions and met with physical therapists to establish standardized approaches to identify and separate fat and muscle borders. Manuals of operation were created for the forefoot, midfoot, and hindfoot to guide the decision making process defining the subcutaneous fat, and intrinsic muscle regions. The manuals used MR images of a foot that were not included in the reliability study. The forefoot was defined as the slice corresponding to the mid-metatarsal, or halfway between the metatarsophalangeal joint (MPJ) and the tarsometatarsal joint of the second metatarsal (Fig. 3a); the midfoot was defined as the slice corresponding to the tarsometatarsal joint of the second metatarsal (Fig. 3b); and the hindfoot was defined as the slice corresponding to the talonavicular joint (Fig. 3c). The plantar side intrinsic foot muscles were separated from the dorsal side muscles by bone in the midfoot and hindfoot, therefore only the plantar side muscle volumes and corresponding subcutaneous fat were segmented and measured (Fig. 3k,l). The subcutaneous fat borders on the medial side of the 1^{st} metatarsal and the lateral side of the 5^{th} metatarsal were defined as just superior to the plantar muscle, perpendicular to the skin surface, and continuing to the cortical shell (Fig. 3h,i). Eleven of the nineteen subject scans did not include the forefoot region, so only the midfoot and hindfoot locations were used in those instances. In total, 46 slices from the nineteen subjects were processed twice by each rater,

with at least 14 days between measurements. Rater 1 averaged 16 days and rater 2 averaged 17.2 days between measurements.

Validity Methods

Phantoms were constructed to test the validity of the program in quantifying lean and adipose tissues using methods similar to those described by Doro et al. (26). Venison was used as a substitute for the intrinsic foot muscles because of its lean nature, and cow fat was used as a substitute for adipose tissue. The proportions of meat and fat were determined by weighing the portions with a scale of 0.1g tolerance. Volumes for the moderate size phantom portions were determined by water displacement, where density estimates were consistent with 1.1 g/cm^3 for the venison and 0.92 g/cm^3 for the fat (27, 28). These constants were used to calculate the volumes of portions that were too small or too large to use the water displacement technique.

The phantoms used in this study consisted of a 2 × 7 plastic pillbox with 14 identical compartments (each approximately 37.5mm long × 22mm wide × 27.5mm deep = 22.7cm^3) filled with known proportions of meat and fat ranging from 0-100% of each type of tissue (26). In addition to the pillbox there were 4 phantoms of approximately 36 cm^3 (≈ 55% fat), 48 cm^3 (≈ 60% fat), 56 cm^3 (≈ 35% fat), and 177 cm^3 (≈ 60% fat). 5 phantoms of pure meat and 4 phantoms of pure fat were also prepared, ranging between 50g and 340g. In total there were twenty-seven phantoms (Fig. 5). The phantoms were scanned and their MR images were converted into the proper formats for the program as described above. The MR scan of the pillbox was obtained where the x-y plane was perpendicular to the long axis of the pillbox. The program automatically determined the threshold for each phantom and calculated the muscle and fat volumes.

Statistical Methods

SPSS (Version 19, Chicago, IL) was used to calculate the intraclass correlation coefficients (ICC) for intra- and inter-rater reliability, and Bland-Altman plots were constructed to illustrate differences between selected repeated measures (29, 30). This report employed the stringent thresholds typical of epidemiological and data analysis studies, where 0.90-1.00 is considered excellent reliability (31, 32). Fisher's Z test was used to determine differences in reliability between scan sequences. The validity of the program was assessed by plotting the observed volume and percent fat proportions of the phantoms of the segmentation program against the predicted volumes and percent fat proportions from water displacement (gold standard). The coefficients of correlation and determination (r and r^2, respectively) were calculated to assess linear dependence and the proportion of the variance of the known volume estimated using the MR method. Mean, standard deviation, and root mean square error (RMSE) of the percent error between the measures were also calculated. As RMSE decreases, predictive power increases, and a RMSE less than 5% represents a standard deviation of predicted-versus-observed error less than 5% of the total volume being measured.

Results

Reliability

Table 2 summarizes the reliability measures of the program methods. Intrarater 1 and intrarater 2 refer to the intrarater reliability of each rater over the two rounds; interrater round 1 and 2 refer to the interrater reliability between the two raters at each round. There were no differences in the reliability values between the two groups of subjects using different MR sequences in 42 of the 48 measures, so ICC values were pooled together. ICC values for each sequence are provided for the 6 measures where a significant difference ($p < 0.05$) between sequence utilization was identified (Table 2). In the forefoot, the ICC values were all above 0.990 for intrarater measures, and above 0.960 for all interrater measures. In the midfoot, all intrarater ICC values were above 0.960 except intrarater 2 had an ICC value of 0.842 for IMAT measures using the proton density weighted sequence. All midfoot interrater ICC values were above 0.950 except for the IMAT interrater round 2, which was 0.808 using the proton density weighted sequence. In the hindfoot, all intrarater and interrater ICC values were above 0.950 except for subcutaneous fat interrater round 1, which was 0.903, and lean muscle rounds 1 and 2 for the proton density weighted sequence, which were 0.928 and 0.910.

Bland-Altman plots were constructed for those measures with ICCs below 0.950 to determine if the relatively lower ICCs were a result of outliers or a bias between the raters (Fig. 6). An outlier in the Bland-Altman plot of the intrarater midfoot IMAT measures is well outside the confidence interval with an error of -0.89 cm^3, and is also present in the Bland-Altman plot of the interrater measures for round 2 (Fig. 6a,b). The Bland-Altman plot of the interrater hindfoot subcutaneous fat measures shows a rater bias of approximately 0.4 cm^3 (Fig. 6c). Interrater hindfoot lean muscle measures show an outlier with an error of -0.9 cm^3 in round 1 and a rater bias of approximately -0.3 cm^3 in round 2 (Fig. 6d,e).

Validity

To help understand validity of the measures, Fig. 7 plots the muscle and fat volumes estimated using the segmentation program versus the water displaced volume measures of the MR phantoms. The observed measures closely matched the predicted measures for all phantoms. Both the muscle-only and fat-only phantoms resulted in r^2 values greater than 0.996 (Fig. 7a,b). The percent error for the muscle-only phantoms had a mean of -0.30, a standard deviation of 3.31, and a RMSE of 3.08. The percent error for the fat-only phantoms had a mean of -1.29, a standard deviation of 3.86, and a RMSE of 3.75. Fig.7c plots percent fat measured by the program against the predicted percent fat as determined by water displacement. The r and r^2 values were both greater than 0.970, and the percent fat error had a mean of 3.11, standard deviation of 3.75, and a RMSE of 4.77.

Discussion

The results show that the segmentation program reliably and validly measured intermuscular adipose tissue (IMAT) and lean muscle tissue in the intrinsic foot muscles. Most ICC values were greater than 0.950, a result of the unique quantitative and objective manner volumes

were calculated. This program was accurate in separating and measuring adipose and lean muscle tissue volumes from MR phantom images ($r^2 > 0.970$ and RMSE < 5%). In addition, the semi-automated program resulted in fast processing times. Both raters, during both rounds of measurements, required 10-15 minutes to process each MR image slice.

A reliable, validated, and quantitative method to measure fat infiltration into foot muscles has been lacking in previous studies. Semi-quantitative scales have been used to assess muscle atrophy on a five point scale based on visual inspection (33). While this method is reliable (ICC = 0.94), fast, and does not require software, it does not quantify volume. Quantitative volume analysis has been performed on the muscles of the foot, but not on the adipose tissue volumes. Anderson et al. and Chang et al. measured total muscle volume based on user defined thresholds, but did not directly quantify IMAT infiltration (34, 35). Neither study reported the reliability or validity of their methods to measure these tissue volumes.

All ICC values indicated excellent reliability except for certain midfoot IMAT measures by rater 2 and hindfoot measures between raters. Fig. 6a shows the Bland-Altman plot of the intrarater midfoot IMAT measures. One outlier is well outside the confidence interval with an error of -0.89 cm^3. This outlier is also present in the Bland-Altman plot of the interrater measures for round 2 (Fig. 6b). Upon review, this error occurred because two different thresholds were chosen for the two rounds of measurements by the rater. This outlier is primarily responsible for the low ICC values rather than other sources of variance. Without this outlier the reliability measures between sequences are no longer significantly different, and pooled together, the ICC value increases to 0.955 for intrarater 2, and to 0.943 for interrater round 2. In regards to the measure of subcutaneous fat in the hindfoot, the Bland-Altman plot of the interrater measures shows a rater bias of approximately 0.4 cm^3 (Fig. 6c). Upon review, the bias appeared to be due to one rater consistently selecting a more superior border of the plantar subcutaneous fat measures on the medial and lateral sides of the foot compared to the other. Fig. 6d,e show the Bland-Altman plots for interrater hindfoot lean muscle measures. An underestimation of lean muscle for one of the subjects resulted in an outlier with an error of -0.9 cm^3 and a bias of approximately -0.3 cm^3 resulting in the lower ICC values. Without this outlier, the reliability measures are no longer significantly different, and pooled together, the ICC values increase to 0.983 for interrater round 1 and 0.969 for interrater round 2. A review of the method manuals by the raters to ensure consistency would likely result in the correction of these errors and improved ICC values.

Validation of the program using fat and lean muscle tissue in the MR phantoms was meant to represent tissue distribution in the foot. The RMSE values indicated the program was accurate not only in measuring pure muscle and pure fat, but in identifying, separating, and measuring muscle and fat volumes when mixed together. Two main sources of error should be considered when using MRI for this application. First, inhomogeneities are inherent to MRI, and partial volume effects occur when multiple tissue types are present in a voxel. Second, tissue orientation and slice thickness lead to volume averaging. The pieces of muscle and fat placed into the pillbox compartments were randomly packed in each compartment, which can result in error due to small air pockets between the materials. This error was minimized by selecting the low intensity threshold to remove voxel intensities less

than 51. In addition, there were only approximately six MR slices for each pillbox compartment which can result in muscle and fat being volume averaged in the 3.5 mm thick slices for the 10 compartments that had muscle and fat mixed (Fig. 6c). The volume averaging errors could have been reduced if all the muscle and fat would have been placed longitudinally in the compartments perpendicular the x-y slices mimicking the foot and reducing the in-slice volume averaging. The remaining four pillbox compartments had either 100% muscle or fat in them and were plotted in Figures 6a and 6b, respectively. Despite these challenges, the program was still able to accurately measure varying proportions of fat in muscle tissue with a RMSE < 5%.

Several other limitations should be considered for the generalizability of these results. MR images of the forefoot were not available in 11 of the 19 subjects because the MR scans did not include the mid-metatarsal region. All forefoot measures had excellent reliability (all ICCs > 0.960), and these values would not be expected to change if the sample size increased. At all three foot locations, the intrinsic foot muscles were segmented as a group and not segmented into individual muscles. Due to their small irregular size, intrinsic foot muscles are always challenging to segment, but especially challenging when infiltrated with IMAT (3, 4, 35). The multiple Gaussian function fitting used to calculate the threshold between muscle and fat tissue is unique to the MR image from each subject and dependent on the parameters of the MR scan. Two different MR scan sequences were used because the subjects were recruited from two different studies. The differences between sequences may not be negligible. The T1 weighted protocol is the better sequence for separating fat from muscle because the proton density sequence could mistake edema for adipose tissue. The proton density sequence was used in the one group of subjects to better optimize tendon images. Variations in scan sequences can introduce additional errors, but the program methods remained highly reproducible in both conditions. Future studies investigating intrinsic foot muscle quality should use a uniform testing protocol without multiple scan sequences to minimize error.

In conclusion, this study is the first to quantify IMAT volumes in the foot through a semi-automatic program, and to assess program reproducibility and validity. The methods are highly reliable and the volumes calculated from the MR phantoms are valid. Subcutaneous fat, lean muscle and adipose tissue in the foot can now be quantified in a reliable and valid way. This program can be applied in future studies investigating the relationship of these foot structures to functions in important pathologies including the neuropathic foot or other musculoskeletal problems.

Acknowledgments

We thank radiologists Drs. Daniel Wessell and Jonathan Baker for MR imaging guidance and expertise. We also thank Dr. Samuel Ward at the University of California San Diego for his assistance in developing methods to test validity.

Grant Support: Contract grant sponsor: NIH, NICHHD, NCMRR; Contract Grant numbers: R21 HD058938-01A1 and T32 HD007434, UL1-RR024992 CTSA, K12 HD055931 from Eunice Kennedy Shriver National Institute of Child Health and Human Development, and KL2 RR024994 – ICTS Multidisciplinary Clinical Research Career Development Program.

References

1. Centers for Disease Control and Prevention. National diabetes fact sheet: national estimates and general information on diabetes and prediabetes in the United States, 2011. Atlanta, GA: U.S. Department of Health and Human Services, Centers for Disease Control and Prevention; 2011. p. 12
2. Andersen H, Gadeberg PC, Brock B, Jakobsen J. Muscular atrophy in diabetic neuropathy: a stereological magnetic resonance imaging study. Diabetologia. 1997; 40(9):1062–1069. [PubMed: 9300243]
3. Bus SA, Yang QX, Wang JH, Smith MB, Wunderlich R, Cavanagh PR. Intrinsic muscle atrophy and toe deformity in the diabetic neuropathic foot: a magnetic resonance imaging study. Diabetes Care. 2002; 25(8):1444–1450. [PubMed: 12145248]
4. Bus SA, Maas M, Michels RPJ, Levi M. Role of intrinsic muscle atrophy in the etiology of claw toe deformity in diabetic neuropathy may not be as straightforward as widely believed. Diabetes Care. 2009; 32(6):1063–1067. [PubMed: 19279305]
5. Holewski JJ, Moss KM, Stess RM, Graf PM, Grunfeld C. Prevalence of foot pathology and lower extremity complications in a diabetic outpatient clinic. J Rehabil Res Dev. 1989; 26(3):35–44. [PubMed: 2666642]
6. Robertson DD, Mueller MJ, Smith KE, Commean PK, Pilgram T, Johnson JE. Structural changes in the forefoot of individuals with diabetes and a prior plantar ulcer. J Bone Joint Surg Am. 2002; 84-A(8):1395–1404. [PubMed: 12177270]
7. Boettcher M, Machann J, Stefan N, et al. Intermuscular adipose tissue (IMAT): association with other adipose tissue compartments and insulin sensitivity. J Magn Reson Imaging. 2009; 29(6): 1340–1345. [PubMed: 19422021]
8. Commean PK, Tuttle LJ, Hastings MK, Strube MJ, Mueller MJ. Magnetic resonance imaging measurement reproducibility for calf muscle and adipose tissue volume. J Magn Reson Imaging. 2011; 34(6):1285–1294. [PubMed: 21964677]
9. Gallagher D, Kuznia P, Heshka S, et al. Adipose tissue in muscle: a novel depot similar in size to visceral adipose tissue. Am J Clin Nutr. 2005; 81(4):903–910. [PubMed: 15817870]
10. Goodpaster BH, Thaete FL, Kelley DE. Thigh adipose tissue distribution is associated with insulin resistance in obesity and in type 2 diabetes mellitus. Am J Clin Nutr. 2000; 71(4):885–892. [PubMed: 10731493]
11. Boulton AJ, Armstrong DG, Albert SF, et al. Comprehensive foot examination and risk assessment: a report of the task force of the foot care interest group of the American diabetes association, with endorsement by the American association of clinical endocrinologists. Diabetes Care. 2008; 31(8):1679–1685. [PubMed: 18663232]
12. Andersen H. Muscular endurance in long-term IDDM patients. Diabetes Care. 1998; 21(4):604–609. [PubMed: 9571350]
13. Andersen H, Stalberg E, Gjerstad MD, Jakobsen J. Association of muscle strength and electrophysiological measures of reinnervation in diabetic neuropathy. Muscle Nerve. 1998; 21(12):1647–1654. [PubMed: 9843064]
14. Hilton TN, Tuttle LJ, Bohnert KL, Mueller MJ, Sinacore DR. Excessive adipose tissue infiltration in skeletal muscle in individuals with obesity, diabetes mellitus, and peripheral neuropathy: association with performance and function. Physical Therapy. 2008; 88(11):1336–1344. [PubMed: 18801853]
15. Tuttle LJ, Sinacore DR, Cade WT, Mueller MJ. Lower physical activity is associated with higher intermuscular adipose tissue in people with type 2 diabetes and peripheral neuropathy. Physical Therapy. 2011; 91(6):923–930. [PubMed: 21474636]
16. Farjoodi P, Mesfin A, Carrino JA, Khanna AJ. Magnetic resonance imaging of the musculoskeletal system: basic science, pulse sequences, and a systematic approach to image interpretation. J Bone Joint Surg Am. 2010; 92A:105–116. [PubMed: 21189247]
17. Broderick BJ, Dessus S, Grace PA, Olaighin G. Technique for the computation of lower leg muscle bulk from magnetic resonance images. Med Eng Phys. 2010; 32(8):926–933. [PubMed: 20655793]

18. Gadeberg P, Andersen H, Jakobsen J. Volume of ankle dorsiflexors and plantar flexors determined with stereological techniques. J Appl Physiol. 1999; 86(5):1670–1675. [PubMed: 10233134]
19. Hussain HK, Chenevert TL, Londy FJ, et al. Hepatic fat fraction: MR imaging for quantitative measurement and display- early experience. Radiology. 2005; 237(3):1048–1055. [PubMed: 16237138]
20. Janssen I, Fortier A, Hudson R, Ross R. Effects of an energy-restrictive diet with or without exercise on abdominal fat, intermuscular fat, and metabolic risk factors in obese women. Diabetes Care. 2002; 25(3):431–438. [PubMed: 11874926]
21. Mathur S, Lott DJ, Senesac C, et al. Age-related differences in lower-limb muscle cross-sectional area and torque production in boys with Duchenne muscular dystrophy. Arch Phys Med Rehabil. 2010; 91(7):1051–1058. [PubMed: 20599043]
22. Ruan XY, Gallagher D, Harris T, et al. Estimating whole-body intermuscular adipose tissue from single cross-sectional magnetic resonance images. J Appl Physiol. 2007; 102(2):748–754. [PubMed: 17053107]
23. Song MY, Ruts E, Kim J, Janumala I, Heymsfield S, Gallagher D. Sarcopenia and increased adipose tissue infiltration of muscle in elderly African American women. Am J Clin Nutr. 2004; 79(5):874–880. [PubMed: 15113728]
24. Stevens JE, Pathare NC, Tillman SM, et al. Relative contributions of muscle activation and muscle size to plantarflexor torque during rehabilitation after immobilization. J Orthop Res. 2006; 24(8): 1729–1736. [PubMed: 16779833]
25. Diamond JE, Mueller MJ, Delitto A, Sinacore DR, Rose SJ. Reliability of a diabetic foot evaluation. Physical Therapy. 1989; 69(10):797–802. [PubMed: 2780806]
26. Doro LC, Ladd B, Hughes RE, Chenevert TL. Validation of an adapted MRI pulse sequence for quantification of fatty infiltration in muscle. Magn Reson Imaging. 2009; 27(6):823–827. [PubMed: 19261424]
27. Anversa P, Hiler B, Ricci R, Guideri G, Olivetti G. Myocyte cell loss and myocyte hypertrophy in the aging rat heart. J Am Coll Cardiol. 1986; 8(6):1441–1448. [PubMed: 2946746]
28. Farvid MS, Ng TW, Chan DC, Barret PH, Watts GF. Association of adiponectin and resistin with adipose tissue compartments, insulin resistance and dyslipidaemia. Diabetes Obes Metab. 2005; 7(4):406–413. [PubMed: 15955127]
29. Bland JM, Altman DG. Statistical methods for assessing agreement between 2 methods of clinical measurement. Lancet. 1986; 1(8476):307–310. [PubMed: 2868172]
30. Shrout PE, Fleiss JL. Intraclass correlations- uses in assessing rater reliability. Psychol Bull. 1979; 86(2):420–428. [PubMed: 18839484]
31. Van Deursen RWM, Sanchez MM, Derr JA, Becker MB, Ulbrecht JS, Cavanagh PR. Vibration perception threshold testing in patients with diabetic neuropathy: ceiling effects and reliability. Diabetic Medicine. 2001; 18(6):469–475. [PubMed: 11472466]
32. Pellis L, Franssen-van Hal NLW, Burema J, Keijer J. The intraclass correlation coefficient applied for evaluation of data correction, labeling methods, and rectal biopsy sampling in DNA microarray experiments. Physiol Genomics. 2003; 16(1):99–106. [PubMed: 14570982]
33. Bus SA, Maas M, Lindeboom R. Reproducibility of foot structure measurements in neuropathic diabetic patients using magnetic resonance imaging. J Magn Reson Imaging. 2006; 24(1):25–32. [PubMed: 16736473]
34. Andersen H, Gjerstad MD, Jakobsen J. Atrophy of foot muscles: a measure of diabetic neuropathy. Diabetes Care. 2004; 27(10):2382–2385. [PubMed: 15451904]
35. Chang R, Kent-Braun JA, Hamill J. Use of MRI for volume estimation of tibialis posterior and plantar intrinsic foot muscles in healthy and chronic plantar fasciitis limbs. Clin Biomech. 2012; 27(5):500–505.

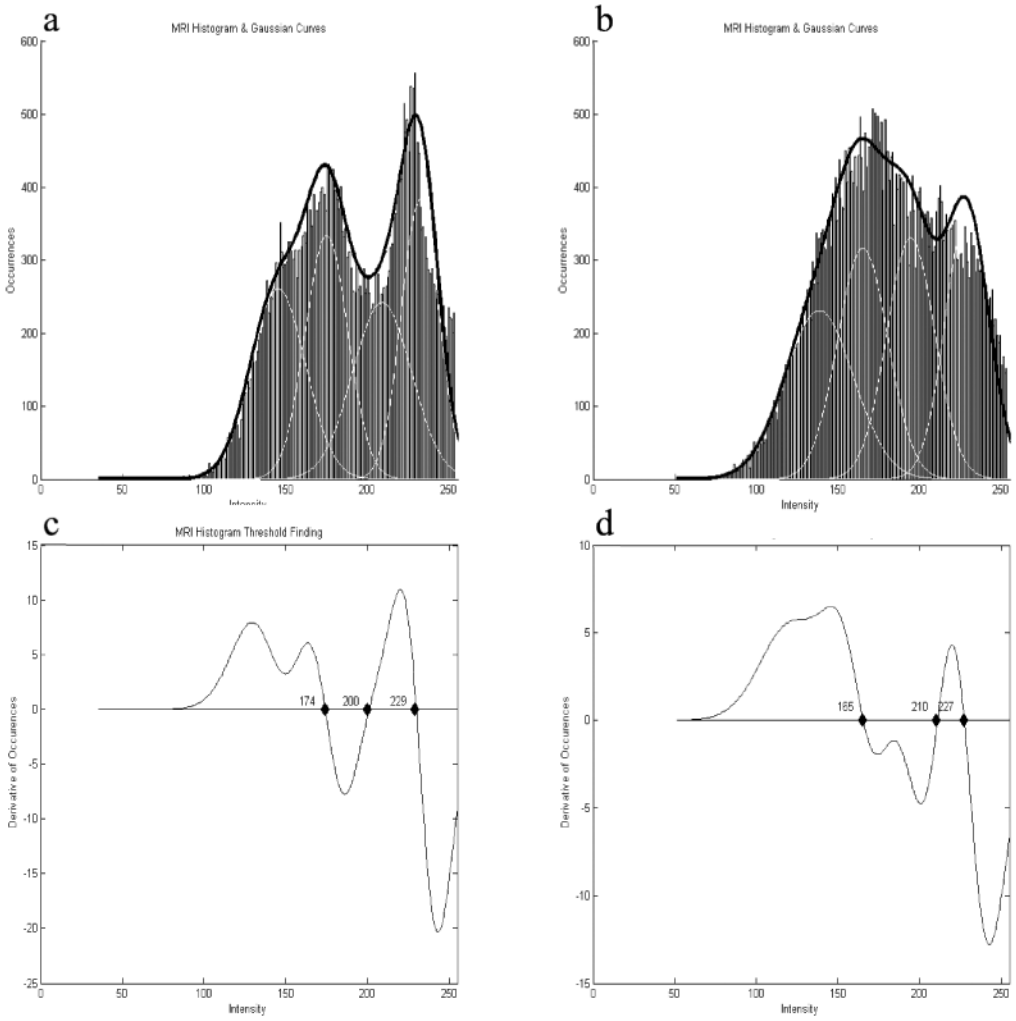

Figure 1.

(a & b) Multiple Gaussian function fitting of signal intensity histogram, and (c & d) corresponding first derivative, where the intensities of 200 and 210 would be selected as the thresholds between adipose tissue and muscle tissue.

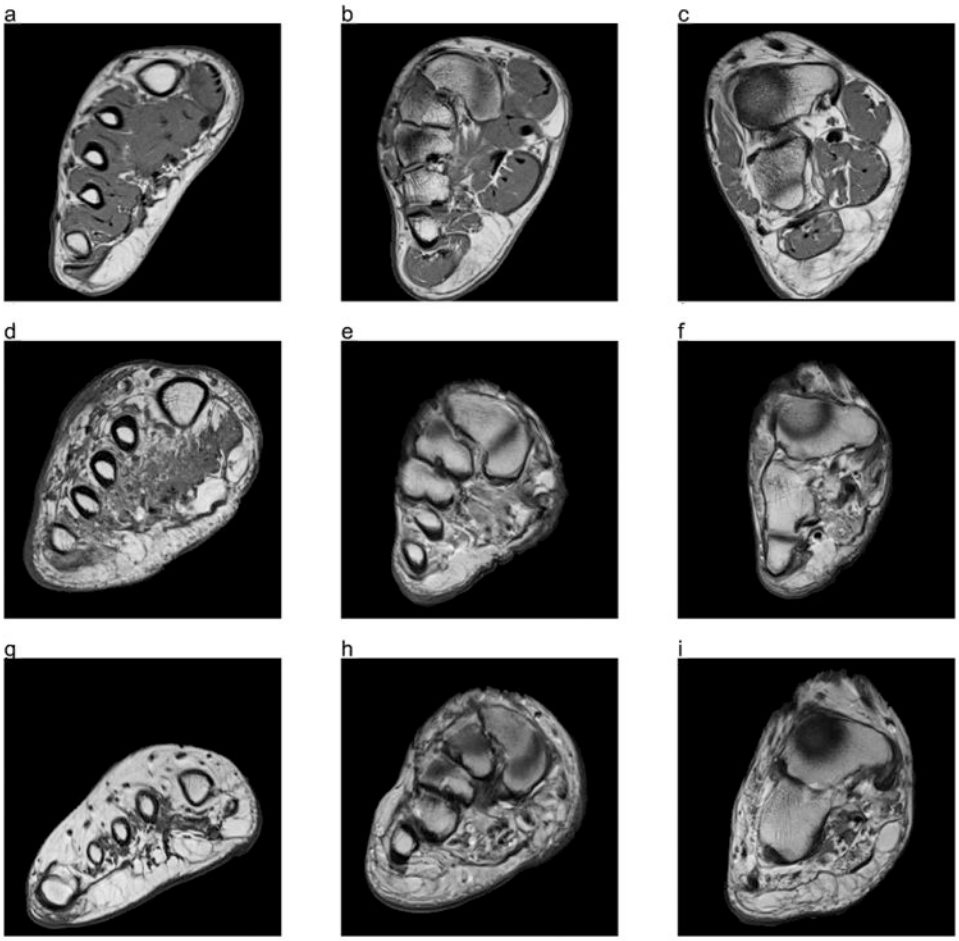

Figure 2.
Comparison of minimal (a-c), moderate (d-f), and severe IMAT infiltration at the fore- (first column), mid- (second column), and hindfoot (third column).

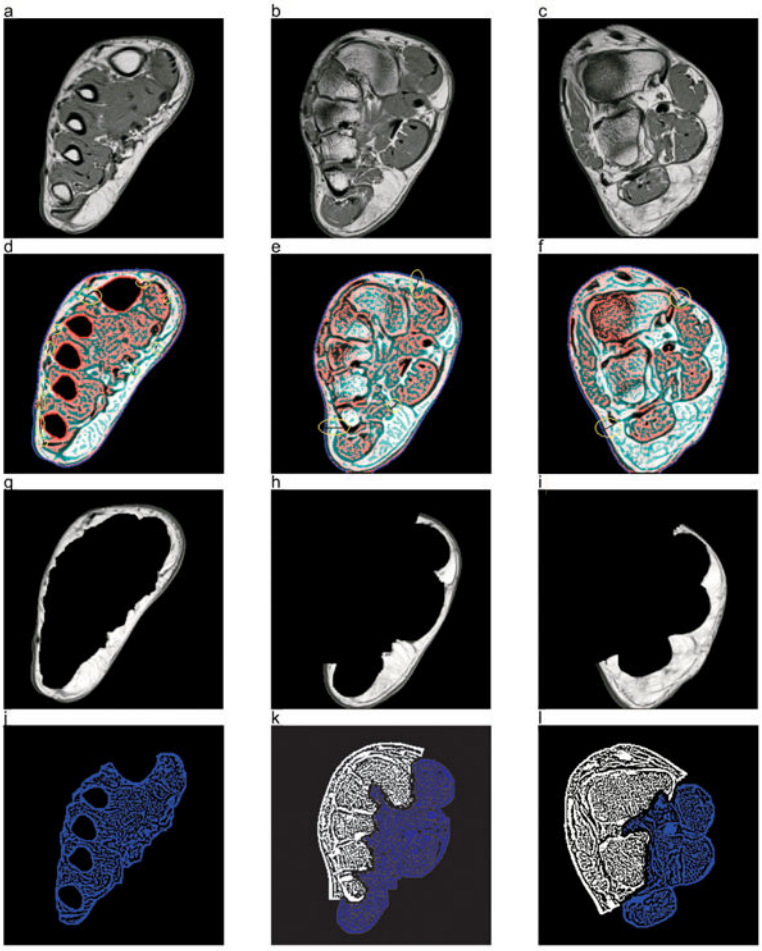

Figure 3.

Segmentation methods of fore-(first column), mid- (second column), and hindfoot (third column). (a-c) MR image; (d-i) separation of subcutaneous fat; (j-l) remaining intrinsic foot muscle.

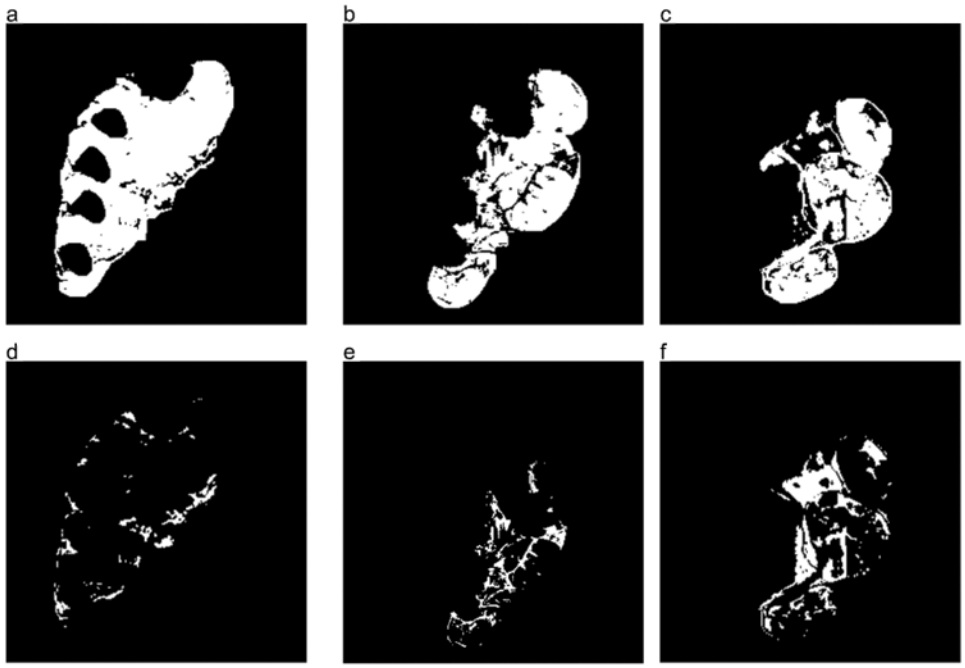

Figure 4.
Muscle (a-c) and fat (d-f) volumes of fore- (first column), mid- (second column), and hindfoot (third column) slices.

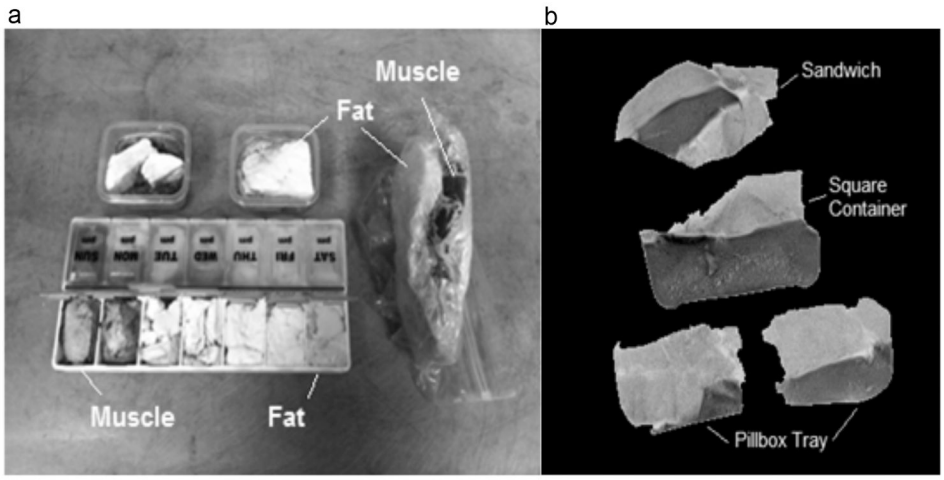

Figure 5.

a: Sample of the MR phantoms constructed, including the square containers, sandwich, and pillbox tray of varying proportions of muscle and fat together, and (b) an MR image of the phantoms. Muscle tissue is dark and fat tissue is bright in both images.

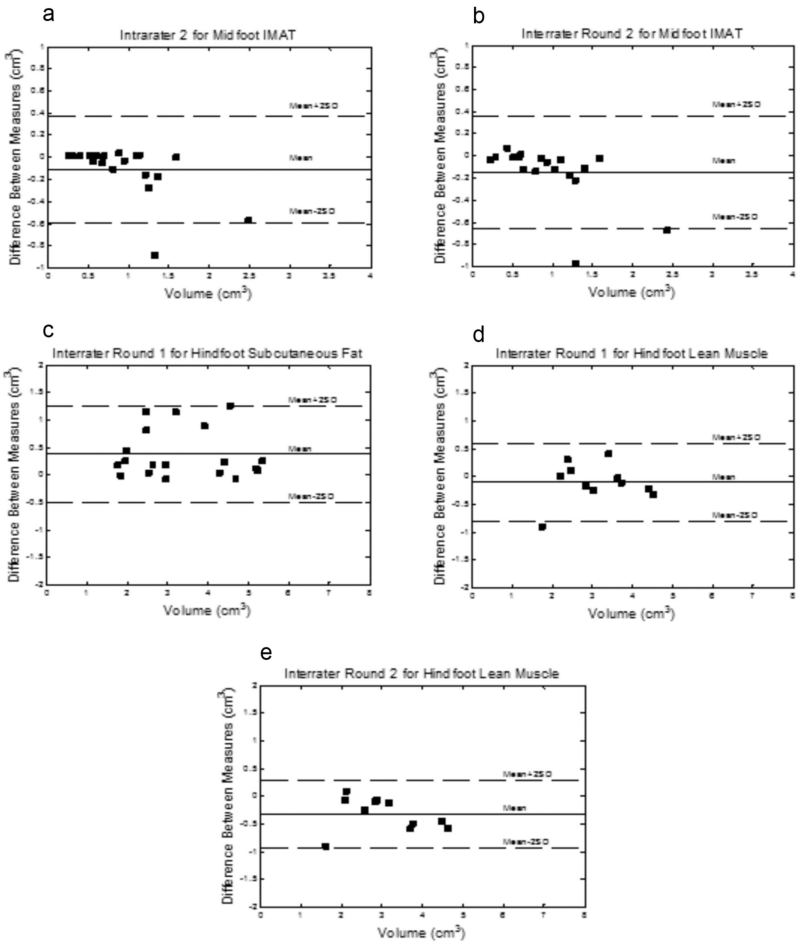

Figure 6.

Bland-Altman plots of selected measures with low ICC values; (a) intrarater 2 for midfoot IMAT, (b) interrater round 2 for midfoot IMAT, (c) interrater round 1 for hindfoot subcutaneous fat, (d) interrater round 1 for hindfoot lean muscle, and (e) interrater round 2 for hindfoot lean muscle.

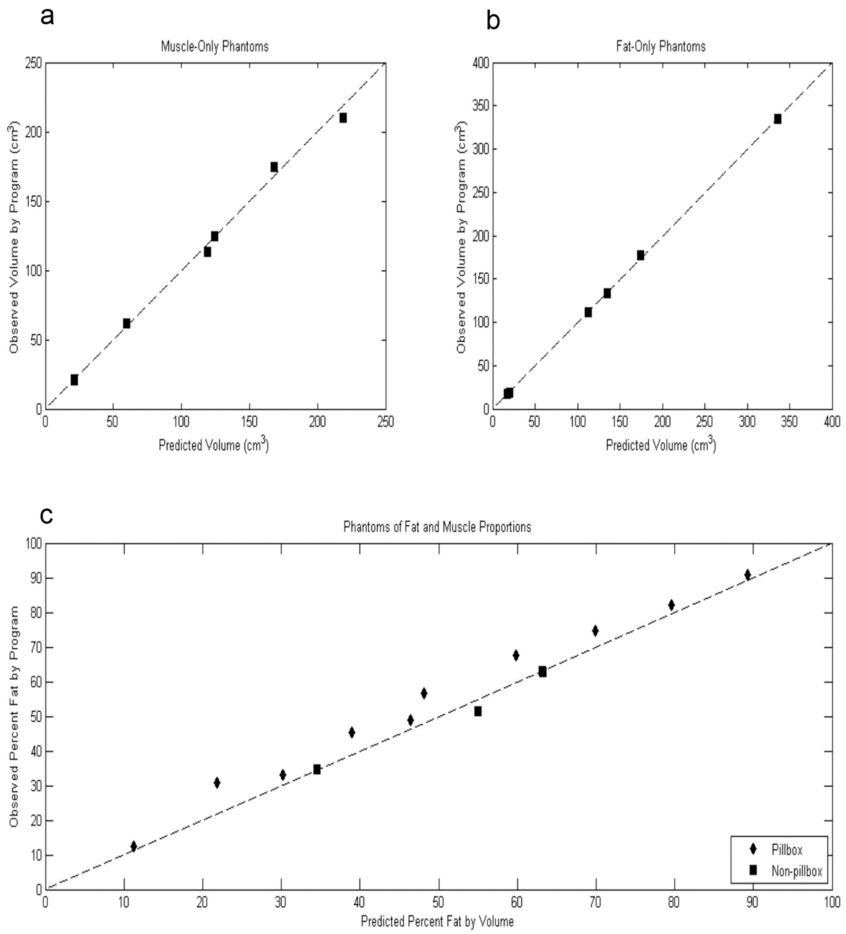

Figure 7.

Observed versus expected volume plots of (a) muscle-only phantoms, (b) fat-only phantoms, and (c) the percent fat by volume of mixed phantoms.

Table 1

Subject Demographics

	DMPN ± deformity	Control
N	6 Female, 6 Male	4 Female, 3 Male
Age (yrs)	57 (12)	53 (12)
Duration of DM (yrs)	18 (10)	
Height (cm)	172 (8)	172 (13)
Weight (kg)	114 (21)	90 (33)
BMI (kg/m^2)	38 (6)	30 (9)

DM = diabetes mellitus; PN = peripheral neuropathy; BMI = body mass index.

Table 2

Intraclass correlation coefficients

Measure	Intrarater 1	Intrarater 2	Interrater Round 1	Interrater Round 2	Mean (SD) Volume (cm^3)
Forefoot (n = 8)					
Whole Slice	1.00	1.00	1.00	1.00	
Subcutaneous Fat	0.995	0.999	0.969	0.977	3.95 (1.30)
Lean Muscle	0.999	0.999	0.998	0.996	3.57 (1.38)
IMAT	0.997	0.999	0.969	0.982	2.19 (1.09)
Midfoot (n = 19)					
Whole Slice	1.00	1.00	1.00	1.00	
Subcutaneous Fat	0.995	0.982	0.992	0.983	2.81 (0.95)
Lean Muscle	0.987	†0.993, ‡0.930	0.973	0.953	3.41 (0.94)
IMAT	0.987	†0.986, ‡0.842	0.988	†0.986, ‡0.808	0.90 (0.49)
Hindfoot (n = 19)					
Whole Slice	1.00	1.00	1.00	1.00	
Subcutaneous Fat	0.992	0.965	0.903	0.969	3.57 (1.26)
Lean Muscle	0.982	0.987	†0.995, ‡0.928	†0.998, ‡0.910	3.22 (1.06)
IMAT	†0.996, ‡0.955	0.985	0.986	0.969	1.16 (0.69)

IMAT, intramuscular adipose tissue; SD, standard deviation. Where scan types are significantly different:

†T1 weighted,

‡proton density weighted.